Research Journal of Applied Sciences, Engineering and Technology 7(15): 3022-3029, 2014
DOI:10.19026/rjaset.7.637
ISSN: 2040-7459; e-ISSN: 2040-7467
© 2014 Maxwell Scientific Publication Corp.
Submitted: December 01, 2012 Accepted: December 31, 2012 Published: April 19, 2014

Research Article

Development of Single-side Magnet Array for Super Paramagnetic Nano-particle Targeting

[1]Wei He, [1]Yongliang Ji, [2]Cong Luo and [1]Zheng Xu
[1]State Key Laboratory of Transmission and Distribution Equipment and System Security and New Technology, The Electrical Engineering College, Chongqing University, Chongqing 400044, China
[2]Children's Hospital of Chongqing Medical University, 136 Zhong Shan Second Road, District of Yu Zhong, Chongqing 400014, China

Abstract: Permanent magnets are interesting for the use in magnetic drug targeting devices. The magnetic fields and forces with distances from magnets have limited the depth of targeting. Producing greater forces at deep depth by optimally designed magnet arrays would allow treatment of a wider class of patients. In this study, we present a design of a permanent magnet array for deep magnetic capture of super paramagnetic iron oxide nano-particles, which consists of an array of 3 individual bar permanent magnet positioned to achieve a reasonably magnitude magnetic field and its gradient within a deeply region. These configurations were simulated with two-dimensional finite-element methods. The super paramagnetic iron oxide nano-particles were adopted Fe_3O_4 particles with diameter 40 nm by chemical co-precipitation method. Performance factors were defined to relate magnetic field force with mass. The field strength and gradient were measured by a Hall probe and agreed well with the simulations.

Keywords: Halbach-like arrays, magnetic drug targeting, magnetostatic application, super paramagnetic iron oxide nano-particles

INTRODUCTION

Super Paramagnetic Iron Oxide Nano-particles (SPIONs) are small synthetic Fe_3O_4 particles with a nano-sized core and an organic or inorganic coating. Unlike bulk ferromagnetic materials, SPIONs have no net magnetic moment until they are placed in an external magnetic field (Mahmoudi *et al*., 2011). In this state, an external magnetic field is able to magnetize the nano-particles, similarly to a paramagnet. However, their magnetic susceptibility is much larger than the one of paramagnets. SPIONs in combination with an external magnetic field allow delivering particles to the desired target area and fixing them at the local site while the medication is released and acts locally (Magnetic Drug Targeting, MDT) (Torchilin, 2000). Therefore, the dosage of the medication can be reduced and the systemic effect of the drugs kept to a minimum. Based on their unique physical, chemical, thermal and mechanical properties, SPIONs demonstrate great potential for various biomedical applications (Kim *et al*., 2001). Magnetic drug targeting has emerged as one of the modern biomedical technologies for drug delivery (Neuberger *et al*., 2005; Nishijima *et al*., 2008) magnetofection (Kosuke *et al*., 2008) and targeted hyperthermia treatment (Gangopadhyay and Gallet, 2005) etc.

Although seemingly straightforward, there are many material and target region properties that complicate the execution of this technique. Material factors such as the physicochemical properties of the SPIONs, target region properties including depth of the target tissue, rate of blood flow and vascular supply, all play a role in determining the effectiveness of this method (Voltairas *et al*., 2002).

Of these factors, the targeting depth is one of the main obstacles to the further application of the technique. Previous attempts to use magnetic nano-particles for MDT give us a vision that externally generated magnetic fields apply relatively small and insufficiently local forces on deep magnetic particles (Jon, 2006; Gangulya *et al*., 2005). The magnitude of magnetic field diminishes with the cube of the distance from field source. Therefore, deep locations are considerably more difficult to target than superficial. It is for this reason that the current studies have been mainly focused on SIOPNs targeting for superficial tissues.

To promote nano-particles retention at targeting sites remote from the magnet surface, the invasive

Corresponding Author: Yongliang Ji, State Key Laboratory of Transmission and Distribution Equipment and System Security and New Technology, The Electrical Engineering College, Chongqing University, Chongqing 400044, China
This work is licensed under a Creative Commons Attribution 4.0 International License (URL: http://creativecommons.org/licenses/by/4.0/).

approaches (Aviles *et al*., 2007, 2008) (e.g., implant magnetized stent, magnetic particles or magnet at the target site) or more strong magnets will be required. An obvious shortcoming of invasive approaches is that the surgery could cause potential harm to patients. Another method, the employ of powerful electromagnets or superconductors could provide stronger magnetic force on magnetic nano-particles (Alexiou *et al*., 2006; Mishima *et al*., 2006). However, the derived magnetic field of these magnets is often unstable. Furthermore, they generally require the use of bulky power suppliers and maintenance equipment.

In order to overcome the shortcomings of the above two methods, this study developed a type of single-side permanent magnet array as a portable magnetic nano-particles targeting magnet device. The magnet array can produce greater magnetic field force on SPIONs at a long distance applied. The design and construction of the single-side magnet array is based on Halbach-like permanent magnet array, of which the magnetic field distribution has obviously single-side feature. A comparison of the newly designed magnet array and single block magnet has been conducted in derived magnetic force, magnetic force efficiency variable and force homogeneity. The results indicate that performance of the newly designed magnet array is improved. Therefore, the magnet arrays presented in the study can be used to target deep focal regions, such as the head, lungs (Plank, 2007), intestines, or liver.

MATERIALS AND METHODS

Materials:

Preparation of super-paramagnetic iron oxide nano-particles: The synthesis of Fe_3O_4 super-paramagnetic nano-particles has been carried out via a controlled chemical co-precipitation reaction. We dissolved a stoichiometric ratio 1:2 ammonium ferrous sulfate hexa-hydrate ($(NH_4)_2$ Fe $(SO_4)_2 \cdot 6H_2O$) and ammonium ferric sulfate odeca-hydrate ((NH_4) Fe $(SO_4)_2 \cdot 12H_2O$) in 200-mL sodium oleate (3%) under vigorous stirring (500 rpm) to prepare ferrite solution as an iron source and heated gently up to 55°C in the meantime. A 100-mL NaOH (6-M) was mixed with 100-mL sodium oleate (1%) as an alkali source and then 200-mL alkali source mixed solution was added drop-wise into 200-mL iron source. After that, the stirring speed was reduced to 150 rpm. The black mixture was then heated at 85°C in a water bath for 30 min.

The precipitate mixture was recovered through siphonage and washed with deionized water to have a pH about 7-8. The overall reaction may be written as shown in Eq. (1) (Gupta and Gupta, 2005):

$$Fe^{2+} + Fe^{3+} + 8OH^- \rightarrow Fe_3O_4 + 4H_2O \quad (1)$$

To control the reaction kinetics, which is strongly related with the oxidation speed of iron species, the synthesis of particles must be done in an oxygen-free environment by passing N_2 gas.

Permanent magnet: The magnet was constructed commercially (99 Magnets, Beijing, China) from three magnetized blocks in a nonmagnetic-conducting stainless steel frame. The magnets are made from nickel-plated sintered NdFeB permanent magnet with Grade-38 (density ρ 7.5×103 kg/m^3, permeability μ 1.049, remanent flux density B_r 1.26 T). The individual block magnets are each 50 mm in length, 4×4 cm in cross section and are magnetized transverse to their long axis. Specifically, more block magnets were bought in advance and the three whose surface magnetization values were the closest to each other were chosen.

Measurement instruments: The hydrodynamic diameter of the nano-particles is determined using dynamic laser scattering in a Particle Size Analyzer (PSA) Rize-2008 from Runzhi Technology Corporation (JiNan, China). The morphology of the SPIONs samples are analyzed using Transmission Electron Microscope (TEM) H-7500 from Hitachi Company (Tokyo, JAPAN). Super-paramagnetic hysteresis curve of the SPIONs is obtained by a Vibrating Sample Magnetometer (VSM, Micro Sense Aquires Sigma Tech, MA, USA) at room temperature. Permanent magnets were measured by a Hall probe (Gauss/Teslameter, F. W. Bell Co., Orlando, FL, USA).

Magnet array construction: The magnet element is carefully inserted into the frame and each magnet is rotated to the correct orientation and finally fixed with three screws. The main difficulty in this process is to introduce the magnet assembly into the frame without breaking or crushing the fragile rare earth magnetic material. When all the blocks are inside the frame and properly aligned and fixed in place, the individual magnet is protected from damage and the structure is mechanically and thermally stable.

Magnetic force on SPIONS: Magnetic force acting on independent SPIONs is determined by using method of dipole moment. Super-paramagnetic nano-particles can be viewed as the single-domain magnetic material, so we can use a point dipole moment mp localized at the center of particle represent magnetic Nano-particle. For a magnetic dipole, we recognize that a uniform magnetic field gives rise to a torque, but no translational action. Therefore, only a non-uniform magnetic field will exert magnetic force on the point magnetic dipole. This magnetic force is governed by the equation:

$$\boldsymbol{F}_m = \left(\left(\boldsymbol{m}_p - \boldsymbol{m}_f\right) g \nabla\right) \boldsymbol{B} \quad (2)$$

where,

m_p = Depends on externally applied magnetic field intensity B at the center of particle

m_f = The respective magnetic moment of the surrounding fluid

Application of the magnetization model of particles based on the self-demagnetization and magnetic saturation would be more accurate, however, the following model is nearly enough for application in the study (Furlani and Ng, 2006). In the case of the magnetic particle suspended in water $m_f = 0$, the total moment on the particle can be written as:

$$\boldsymbol{m}_p = V_p \frac{\bar{\chi}}{\mu_0} \boldsymbol{B} \tag{3}$$

where, V_p is the volume of the spherical particle, $\bar{\chi}$ is corrected susceptibility of the particle. The geometry of the particle also affects its ability to magnetize in an external magnetic field (Baselt *et al*., 1998). For spherical particles, the shape corrected susceptibility $\bar{\chi} = 3\chi/(\chi + 3)$.

According to Eq. (3), (2) can be reformulated:

$$\boldsymbol{F}_m = \frac{V_p \bar{\chi}}{\mu_0} (\boldsymbol{B} \mathrm{g} \nabla) \boldsymbol{B} \tag{4}$$

Equation (4) indicates that in order to achieve significant magnetic force, the particles should have large volumes and susceptibility and the magnet array system should generate large the strength B and the gradient of the magnetic field ∇ B meanwhile.

In order to facilitate the design of MDT magnet arrays, simplified and direct factor is necessary to be derived instead of the above two variables. Provided there is no time-varying electric field or currents in the medium, we can apply the Maxwell equation $\nabla \times B = 0$ to the following mathematical identity:

$$\nabla(\boldsymbol{B} \mathrm{g} \boldsymbol{B}) = 2\boldsymbol{B} \times (\nabla \times \boldsymbol{B}) + 2(\boldsymbol{B} \mathrm{g} \nabla)\boldsymbol{B} = 2(\boldsymbol{B} \mathrm{g} \nabla)\boldsymbol{B} \tag{5}$$

Thus, we can obtain a more intuitive form of Eq. (4):

$$\boldsymbol{F}_m = V_p \bar{\chi} \nabla \left(\frac{B^2}{2\mu_0} \right) \text{ or } \boldsymbol{F}_m = V_p \bar{\chi} \nabla \left(\frac{1}{2} \boldsymbol{B} \mathrm{g} \boldsymbol{H} \right) \tag{6}$$

In Eq. (6) the magnetic force is related to the differential of the magnetostatic field energy density, BgH/2. The relation states that the force on a single particle is proportional to its volume and the gradient of the magnetic field energy density and shows that a spatially varying magnetic field is required to create a magnetic force. Thus, in order to obtain greater the force experienced by a given particle, the gradient of the magnetic field squared must be increased. This is the only term controlled by the magnet design; all other terms depend on the size and material properties of the particles.

Methodology:

Calculation precondition preparation: The motion of SPIONs within the target tissue is mainly controlled by the combination of magnetic force and a hemodynamic drag force due to the surrounding fluid flow. In order to efficiently retain the particles at the target site, the attractive magnetic forces exerted on the particles must overcome the drag forces produced by the fluid flow. The magnetic force on a particle of diameter d is proportional to third power diameter (d^3), while the drag force F_d, according to Stoke's law Eq. (7), is proportional to diameter (d):

$$F_d = 3\pi\mu d \left(v - v_p \right) \tag{7}$$

where,

μ = The dynamic viscosity of the fluid medium
d = The diameter of the particles
v = The fluid medium flow velocity
v_p = The velocity of the particles

Based upon this principle, large particles are more easily retained with an external magnet. To be able to focus on designing high performance delivery and targeting magnet for SPIONs, in this study, our methodology is based on reasonable restriction that all nano-particles are in a fixed flow viscous environment. In other words, the drag force of the particles is invariable for the two type of magnets compared in the work. With the restriction, we could investigate the external magnetic field applied on nano-particles generated by different type magnets merely and ignore the influence of different fluid environment. Thus the clear comparison of magnetic force as retention requirement of nano-particles could be achieved.

General requirements for magnetic field: Preliminary theoretical investigations of the hydrodynamic conditions of magnetic Nano-particle targeting and estimations from experimental work indicate that for most magnetite-based carriers, flux densities at the target site must be of the order of 0.2 T with field gradients of approximately 8 T/m for femoral arteries and greater than 100 T/m for carotid arteries (Kosuke *et al*., 2008).

Simulation and measurement: Magnetic force was determined using the Eq. (6) and properties of magnetic nano-material. The estimates of gradient of the magnetic field energy density in Eq. (6) were obtained by a two-step procedure for various magnetic arrays.

First step, the remanent flux density B was calculated using the Finite Element Analysis (FEA) scheme. The linear magnetic constitutive relation was used for the FEA. The remanent flux densities were applied to the excitation part of the Galerkin's formulation in the two-dimensional Cartesian case to analyze the magnetic field numerically:

$$\iint_{\Omega} \frac{1}{\mu}\left(\frac{\partial A_z}{\partial x}\frac{\partial N_l}{\partial x}+\frac{\partial A_z}{\partial y}\frac{\partial N_l}{\partial y}\right)dxdy - \iint_{\Omega} \frac{1}{\mu}\left(B_{r,x}\frac{\partial N_l}{\partial y}-B_{r,y}\frac{\partial N_l}{\partial x}\right)dxdy = 0 \quad (8)$$

where,

A_z = The magnetic vector potential
μ = The permeability
N_l = The interpolation function which is also known as the shape function

Second step, the gradient of the magnetic field energy density could be yielded by the dot product of magnetic flux density B and magnetic field H data.

The static magnetic flux density profile on and above the top of the magnet was measured using a Hall probe fixed on a home-assembled program controlled 3D translation stage. Measured field profiles were plotted using the graphing and data analysis software package Origin v8.0 (OriginLabs, Northampton, MA, USA).

RESULTS

PSA measurement shows that the mean size of magnetic nano-particles is around 40 nm, which is also proven by TEM image (Fig. 1). The magnetic hysteresis curve of the particles is shown in Fig. 2. For the particles, the specific saturation magnetization M_S = 8.223 emu/g, which is defined here as the intercept at $1/H = 0$ of the straight line obtained by a linear fit to the data points for $H \geq 1.9\times104$ Oe. The remanence M_r is 0.019 emu/g and the coercivity H_C is 1.7 Oe (Fig. 2). No coercivity or remanence could be observed for the sample suggesting that Fe_3O_4 iron oxide nano-particles have super-paramagnetic properties.

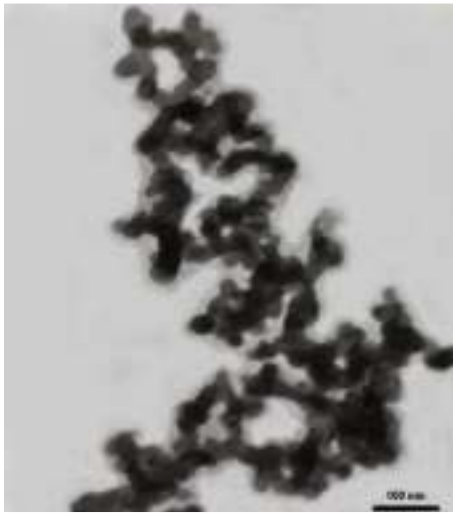

Fig. 1: TEM micrograph of synthesized super-paramagnetic iron oxide nano-particles

The FEA simulation and measured results for magnitude of magnetic field and magnetic field gradient are shown in Fig. 3a and b for the Halbach-like magnet. The magnitude of magnetic field and its gradient are 0.28 T and 9.1 T/m at the distance of 3 cm. According to the trapping requirement of SPIONs in pervious section, the values could reach the requirement general MDT applications.

The goal is to maximize magnetic pull forces along the negative direction of vertical axis and, thus, the focus is solely on the vertical component of F_m, i.e., $-|F_m|_z$. In Fig. 4a and b the negative vertical component of magnetic force for the simple magnet and

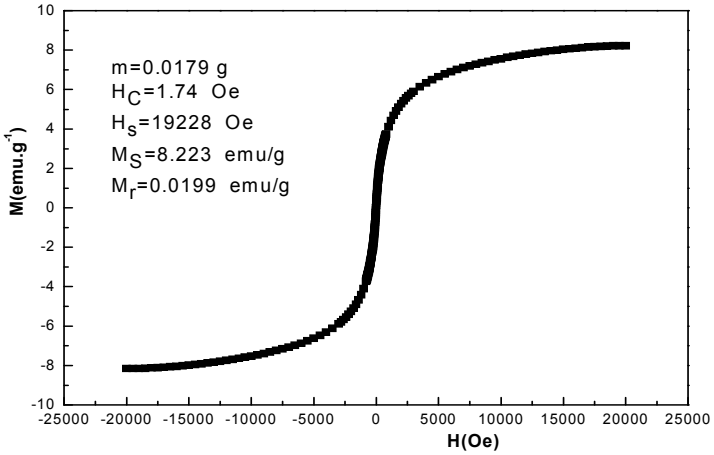

Fig. 2: The super-paramagnetic magnetization curve of synthesized SPIONs

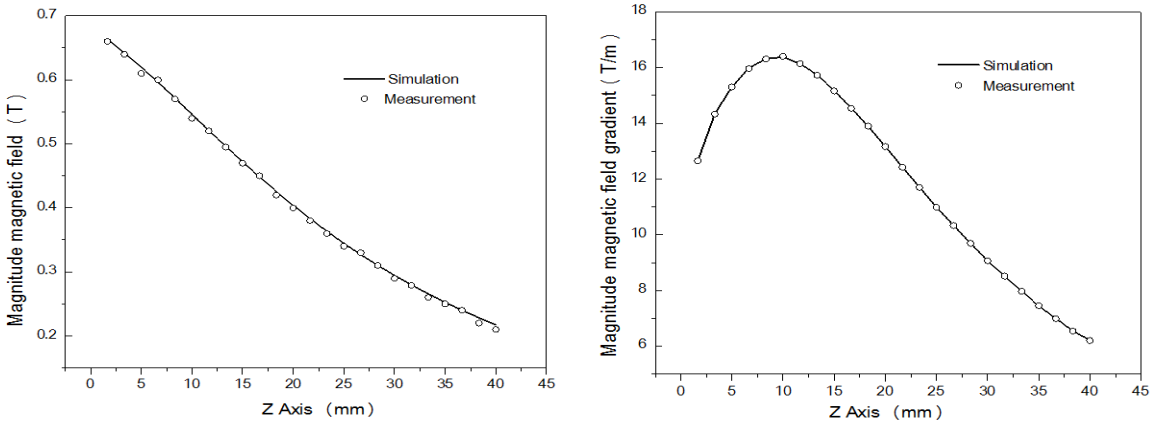

(a) (b)

Fig. 3: (a) Simulation and measured magnitude of magnetic flux density of halbach-like magnet along the line 0-4 cm from the centre of magnet top face, (b) simulation and measured magnitude of magnetic flux density gradient of halbach-like magnet along the line 0-4 cm from the centre of magnet top face

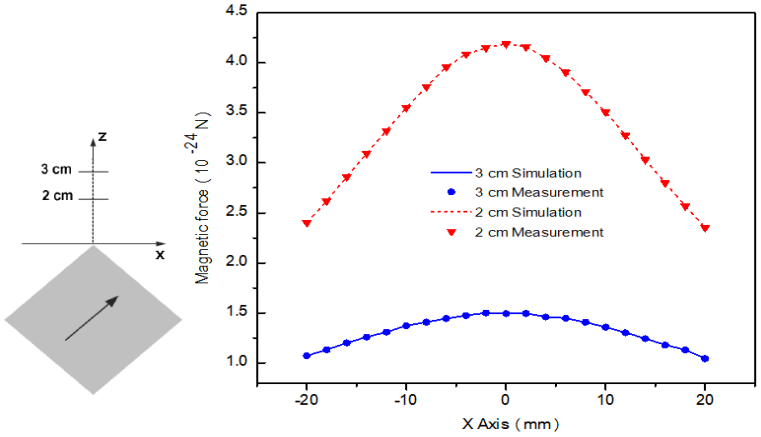

(a)

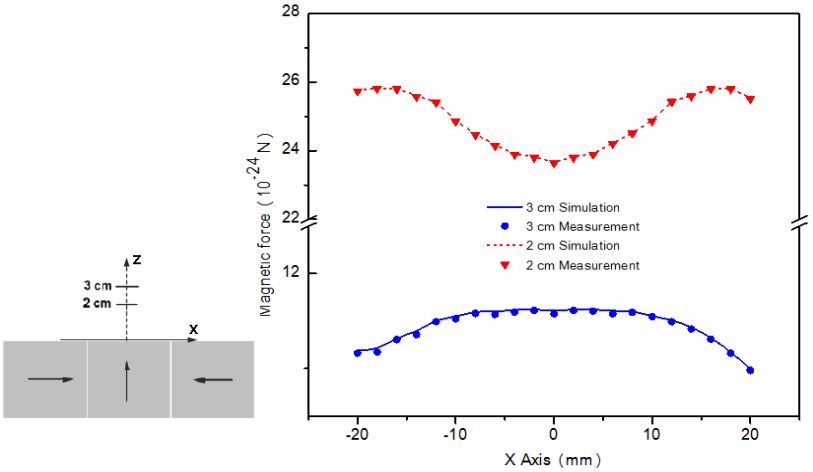

(b)

Fig. 4: (a) The negative vertical component of magnetic pull forces for simple magnet at the location 2 and 3 cm, (b) the negative vertical component of magnetic pull force for halbach-like magnet at the location 2 and 3 cm

Halbach-like magnet were plotted at the location 2 and 3 cm, respectively. Based on the comparisons, the magnetic force on nano-particles duo to Halbach-like magnet is about ten times larger than that of simple magnet.

DISCUSSION

While designing a MDT magnet one must consider several factors and perform a careful tradeoff analysis to arrive at the optimal instrument for the application of interest. So, this deals with a question about how to evaluate the performance of MDT permanent magnet array system.

First, the external guiding magnet should provide high and scalable magnetic navigating force around the application site and inside the area for attracting and retaining the magnetic drug particles. Obviously, the magnetic force generated from magnet is increased with bigger volume and weight of magnet array. However, it is necessary to select suitable and optimized magnet instead of bigger and heavier ones. For the purpose, the magnetic force efficiency variable η:

$$\eta = \frac{|\boldsymbol{F}_m|}{Weight} \tag{9}$$

is proposed to evaluate the magnetic force-weight property of magnet arrays. Above the italic Weight is the total weight of magnet arrays. Expression (9) illustrates that the ability to exert magnetic force of per-unit-weight magnet arrays on SPIONs. Based on the Expression (9) the variable η is high for stronger magnetic force yielded by per-unit-weight magnet arrays. The magnet array which has larger η value has better force-weight property and magnetic materials utilization than the ones have less value.

In Fig. 5 the comparison of magnetic force efficiency variable along with the Z-axis for the simple magnet and Halbach-like magnet was presented. Specifically, the simple magnet is identical with element block magnet of Halbach-like magnet array (same size and material). The force efficiency variable could evaluate diverse permanent magnet systems for MDT as a key consideration. Halbach-like array is an effective geometry optimizing the force/mass ratio and should be pursued when the size or weight of the magnet needs to be minimized for patient comfort.

Furthermore, another property interested in a MDT experiment is the transverse homogeneity of magnetic force exert on particles at concerned distance around the target. The reason is that effective drug therapies need to achieve a certain drug concentration in the lesion location. Therefore, high transverse homogeneity means that there is greater magnetic valid region for SPIONs retention at the interesting therapeutic areas. Hence, a second performance factor δ is defined to take this into account for evaluation different magnet arrays. The calculation of homogeneity for magnetic force exerted on microsphere employs the expression (10):

$$\delta = 2\left(\frac{F_{m\max} - F_{m\min}}{F_{m\max} + F_{m\min}}\right) \tag{10}$$

Expression (10) indicates that the smaller δ provide higher homogeneity of magnetic force and small difference for the magnetic force in a region give rise to increase of homogeneity. According to the measurement results inside the half centimeter of horizontal around 3 cm, the homogeneity for the simple magnet and Halbach-like magnet is 280±1 and 10±1 parts per ten-thousand (pptt, 10^{-4}). The homogeneity could not be calculated with such precision. In fact the

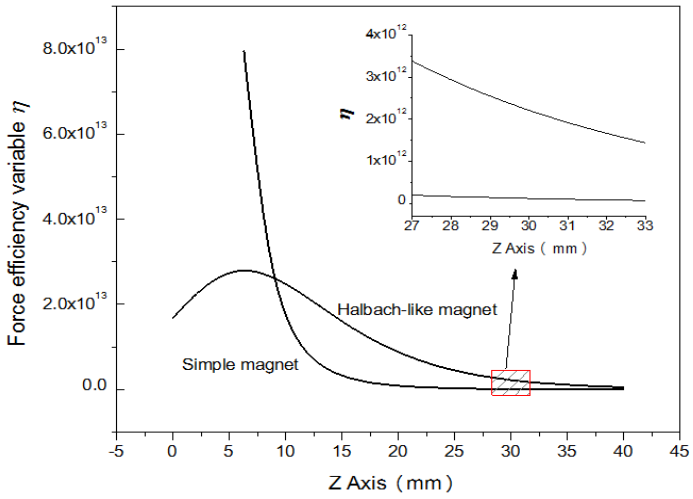

Fig. 5: Graph of magnetic force efficiency variable for halbach-like array and simple magnet. Inset shows the local detail around 30 mm on the horizontal coordinate

realization shows a difference in homogeneity of 1 pptt. This difference is caused by mechanical tolerances (±100 μm), in the axial position (±500 μm) and quality of the material (magnetization and homogeneity).

According to the discussion in previous section, the Halbach-like magnet array has considerably greater force efficiency and better transverse uniform spatial distributions of magnetic force than simple magnet array on magnetic nano-particles.

There are numerous and complex hydrodynamic and physiological factors influence the control of real magnetic drug nano-particles. This is a complex problem that requires the parameters about characteristics of blood flow (such as velocity and viscosity), materials properties (particle size distribution and magnetization characteristics), particle-particle interaction (agglomeration) and complex particle-wall interactions including extravasation (Goodwin *et al*., 2001). However, the calculation of the distribution of magnetic force on a SPION provides useful insight into the relative effectiveness of magnet arrangements for drug-targeting applications. In addition, the method can provide an instruction to design and evaluation of the MDT-magnet system.

CONCLUSION

A portable open magnet array for deep region magnetic drug targeting has been established and evaluated. This newly designed magnet system is quite capable of being used for retention magnetic nano-particles in relatively deeper positions inside the body. The comparison calculations clearly illustrate advantages of Halbach-like magnet array relative to simple geometry array, both in terms of three considerations, magnetic force F_m, magnetic force efficiency variable η and homogeneity δ, which can be achieved. The remarkable uniformity and magnitude of the forces exerted by newly designed Halbach-like arrays suggests that in many situations they may represent an ideal geometry for both experimental and clinical applications.

ACKNOWLEDGMENT

This study was supported in part by the Key Research Projects of Chongqing Science and Technology Commission under Grant CSTC 2011GGB1004 and the Fundamental Research Funds for the Central Universities under Grant CDJZR10150021.

REFERENCES

Alexiou, C., D. Diehl, P. Henninger and H. Weber, 2006. A high field gradient magnet for magnetic drug targeting. IEEE T. Appl. Supercon., 16(2): 1527-1530.

Aviles, M.O., A.D. Ebner and J.A. Ritter, 2008. Implant assisted-magnetic drug targeting: Comparison of in vitro experiments with theory. J. Magn. Magn. Mater., 320(21): 2704-2713.

Aviles, M.O., H. Chen, A.D. Ebner, A.J. Rosengart, M.D. Kaminski *et al*., 2007. *In vitro* study of ferromagnetic stents for implant assisted-magnetic drug targeting. J. Magn. Magn. Mater., 311: 306-311.

Baselt, D.R., G.U. Lee, M. Natesan, S.W. Metzger, P.E. Sheehan and R.J. Colton, 1998. A biosensor based on magnetoresistance technology. Biosens. Bioelectron., 13: 731-739.

Furlani, E.P. and K.C. Ng, 2006. Analytical model of magnetic Nano-particle transport and capture in the microvasculature. Phys. Rev. E., 73(6): 1-10.

Gangopadhyay, P. and S. Gallet, 2005. Novel superparamagnetic core (Shell) nano-particles for magnetic targeted drug delivery and hyperthermia treatment. IEEE T. Magn., 41: 4194-4196.

Gangulya, R., A.P. Gaind, S. Sen and I.K. Puri, 2005. Analyzing Ferro fluid transport for magnetic drug targeting. J. Magn. Magn. Mater., 289: 331-334.

Goodwin, S.C., C.A. Bittner, C.L. Peterson and G. Wong, 2001. Single dose toxicity study of hepatic intra-arterial infusion of doxorubicin coupled to a novel magnetically targeted drug carrier. Toxicol. Sci., 60(1): 177-183.

Gupta, A.K. and M. Gupta, 2005. Synthesis and surface engineering of iron oxide nano-particles for biomedical applications. Biomaterials, 26: 3995-4021.

Jon, D., 2006. Magnetic nano-particles for drug delivery. Drug Dev. Res., 67: 55-60.

Kim, D.K., Y. Zhang, W. Voit, K.V. Rao, J. Kehr, B. Bjelke and M. Muhammed, 2001. Superparamagnetic iron oxide nano-particles for bio-medical applications. Scripta Mater., 44: 1713-1717.

Kosuke, I., K. Tamayo and I. Akira, 2008. Plasmid DNA transfection using magnetite cationic liposomes for construction of multilayered gene-engineered cell sheet. Biotechnol. Bioeng., 100: 168-176.

Mahmoudi, M., S. Sant, B. Wang, S. Laurente and T. Sen, 2011. Super Paramagnetic Iron Oxide Nano-particles (SPIONs): Development, surface modification and applications in chemotherapy. Adv. Drug Deliver. Rev., 63*:* 24-46.

Mishima, F., S.I. Takeda, Y. Izumi and S. Nishijima, 2006. Three dimensional motion control system of ferromagnetic particles for magnetically targeted drug delivery systems. IEEE T. Appl. Supercon., 16(2): 1539-1542.

Neuberger, T., B. Schppf, H. Hofmann, M. Hofmann and B. Von Rechenberg, 2005. Superparamagnetic nano-particles for biomedical applications: Possibilities and limitations of a new drug delivery system. J. Magn. Magn. Mater., 293: 483-496.

Nishijima, S., S.I. Takeda and F. Mishima, 2008. A study of magnetic drug delivery system using bulk high temperature superconducting magnet. IEEE T. Appl. Supercon., 18(2): 874-877.

Plank, C., 2007. Nanomagnetosols: Magnetism opens up new perspectives for targeted aerosol delivery to the lung. Trends Biotechnol., 26: 59-63.

Torchilin, V.P., 2000. Drug targeting. Eur. J. Pharm. Sci., 11: 81-91.

Voltairas, P.A., D.I. Fotiadis and L.K. Michalis, 2002. Hydrodynamics of magnetic drug targeting. J. Biomech., 35: 813-821.